Journal of Ovonic Research Vol. 8, No. 2, March - April 2012, p. 21 - 27

INFLUENCE OF ANNEALING ON STRUCTURAL AND OPTICAL PROPERTIES OF GERMANIUM QUANTUM DOTS

ALIREZA SAMAVATI[a*], SIB KRISHNA GHOSHAL[b], ZULKAFLI OTHAMAN[a]
[a]*Ibn Sina Institute for Fundamental Science Studies, Universiti Teknologi Malaysia, 81310 Skudai, Johor Baharu, Malaysia*
[b]*Advanced Optical Material Research Group, Department of Physics, Faculty of Science, Universiti Teknologi Malaysia, 81310 UTM Skudai, Johor, Malaysia,* 81310 Skudai, Johor Baharu, Malaysia

Ge nanodots are grown on a Si(100) substrate by radio frequency magnetron sputtering deposition technique. The role of annealing temperature on structural and optical properties is studied. The formation of nanodots is confirmed by X-ray diffraction pattern and the particle size is estimated to be ~ 6.5 to 8.5 nm. The structure and optical characterizations are made using, Energy dispersive X-ray diffraction, field emission scanning electron microscopy, atomic force microscopy, photoluminescence and Raman spectroscopy. The interface intermixing and the size of the nanodots are determined from Raman spectra and field emission scanning electron micrograph. Root mean square roughness and number density are found to be strongly influenced by annealing temperature. Photoluminescence spectra shows the strong emission peak at 3.21 eV accompanied by two weaker peaks at around 2.85 and 4.13 eV in the visible region. The red shift of the strong peak ~ 0.05 eV is attributed to the effect of quantum confinement.

(Received February 6, 2012; Accepted March 1, 2012)

*Keywords***:** Quantum dot; Photoluminescence; Raman spectroscopy; Semiconductor

1. Introduction

Conversion of bulk structures into nanoscale involves the remarkable change in physical properties of materials. It provides the possibility of observing novel behavior such as size dependent structural and optical properties. The influence of the growth procedure and the corresponding mechanism of self-assembly (Stranski-Krastanov) of Ge nanostructure on Si substrate are of particular interest for obtaining highly monodisperse nanostructure for semiconductors optoelectronic devices application.

Magnetron sputtering method due to its high deposition rate and safety currently becomes the most popular commercially viable methods for fabrication the Ge\Si semiconductor heterostructure [1, 2]. The Ge and GeO_2 nanocrystals luminescence is observed around 3.1 eV and the strongest PL intensity evidenced for larger nanocrystals [3]. The PL spectra of Ge nanostructure having size between 2 and 9 nm can be viewed as a combination of three peaks at around 1.9, 2.3 and 3.0 eV as reported by Kartopu et al [4]. The Ge islands having height from 1 to 2 nm and widths from 40 to 50 nm are fabricated by Thanh et al in which the observed broadening in the PL spectra are correlated to the broad dispersion in the nanostructure size distribution [5]. Interestingly, the thermal annealing strongly influences the structural, optical (~ 0.25 eV shift for band gap energy and 2 cm^{-1} Raman's signal shift due to changing the particle size) and electrical properties of Ge QDs [6].

* Corresponding author : Alireza.samavati@yahoo.com

Few studies exist on sputtering and the effect of annealing in changing the size and optical behavior of Ge quantum dots (QDs) is far from being understood. However, controlling the light emitting behavior require careful fabrication of such a nanostructure. This research is targeted to fulfill this perspective by providing an efficient and easy fabrication method using sputtering. The results on structural and optical characterizations are presented.

2. Experimental Procedures

Ge QDs are sputtered on Si(100) at 400 ^{o}C substrate temperature using HVC penta vacuum system. The target is 3 inches pure Ge (99.99%) disc. Before the substrates are loaded into the deposition chamber, a standard cleaning process is undertaken in which Si(100) is first etched with 5% HF for 2 min and then cleaned ultrasonically in deionized water. Prior to the deposition, the targets are pre-sputtered for 2 min with closed shutter to remove the presence of surface contamination if any. The working pressure, RF power and Ar flow are fixed at 6.5×10^{-3} torr, 100 W and 10 Sccm respectively (designated as sample A). Rapid thermal annealing (Anneal sys, AS-One 150) is carried out in N_2 ambient in 120 sec (designated as sample B). The surface morphology and structural analysis are investigated by, AFM at room temperature FESEM and XRD. The PL spectra are recorded at room temperature, using the (Perkin Elmer Ls 55) Luminescence Spectrometer under 239 nm excitation sources. The Raman scattering experiments were performed using 50 mW lasers power.

3. Results and discussion

The EDX spectra from samples A and B are shown in figs. 1a and 1b respectively that confirms the formation of Ge QDs on Si substrate. The presence of oxygen peak is due to the surface passivation and suggests the possibility of GeO present in the structure. The intense Ge peak at EDX spectra can be observed for sample B due to larger size Ge QDs along (100) direction. The weaker peak for Ge is attributed to the growth of Ge crystals along the (111) direction.

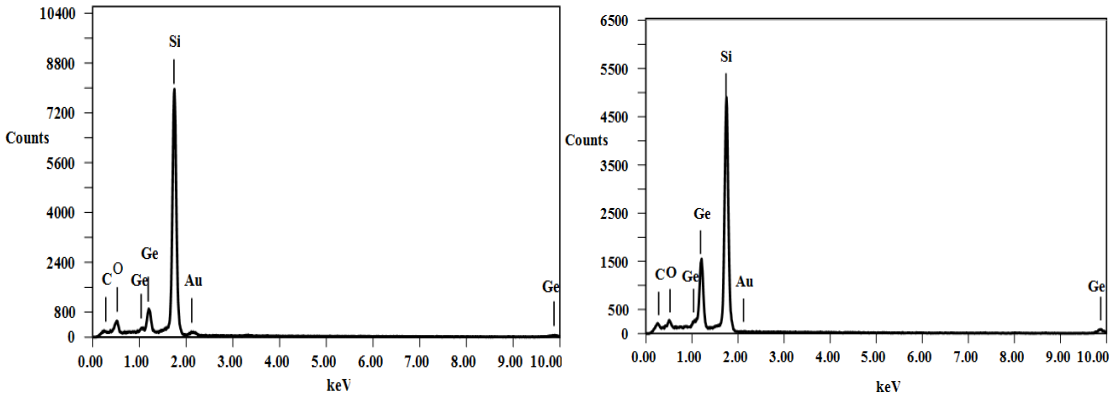

Fig. 1. EDX spectra for sample A(a) and B(b)

Fig. 2(a) and (b) shows the FESEM images of the Ge QDs before and after the annealing at 700 ^{o}C respectively illustrating the presence of Ge nanodots, with particle size lies in the range of 7–14 nm in agreement with the XRD results.

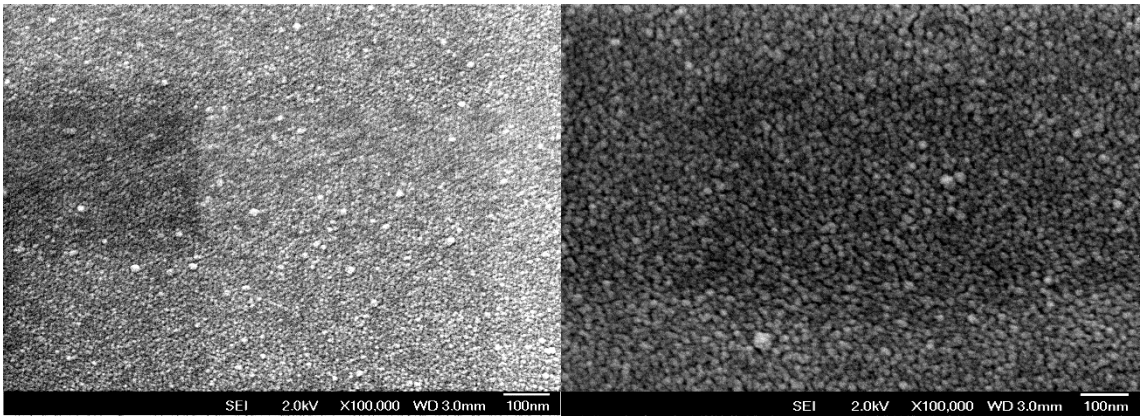

Fig. 2. FESEM images for samples A before (a) and B after (b) annealing.

The fluctuation of heights of Ge QDs is more apparent in the lateral diagram of height distribution as can be seen in fig.3 obtained from AFM topographic images. The AFM lateral diagram images clearly illustrate the existence of Ge dots having heights between 2 to 4 nm. Thermal annealing can lead to a rearrangement of the inner structure of the Ge/Si nanostructure leading to the formation larger nanodots size and converting the shape of QDs from metastable pyramid to dome-like structure as clearly seen from fig.3. This observation is attributed to the thermal diffusion and the nucleation mechanism of the growth processes.

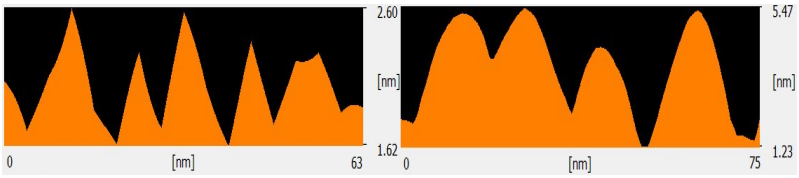

Fig.3 Lateral diagram of height fluctuation from AFM for sample A before (a) and B after (b) annealing.

Increasing the temperature from room temperature to 700 ^{o}C coarsen majority of the smaller particle to form larger particle and thereby reduce the density drastically. This rapid decrement in density can be understood by the kinetics of the growth mechanism that occurs via thermal diffusion. Fig. 4 shows the root mean square (RMS) roughness and the number density of samples revealed by

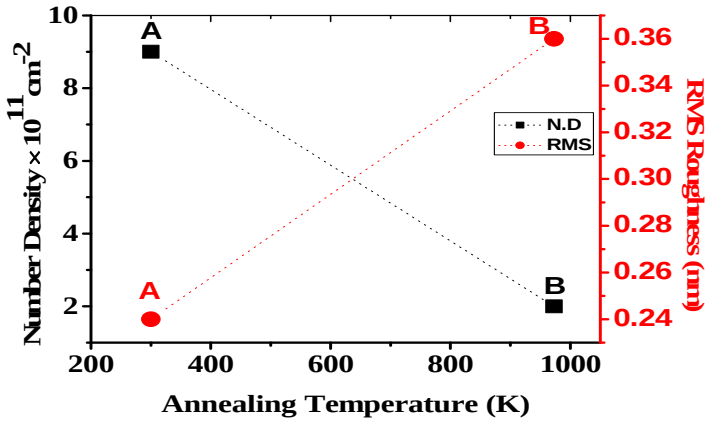

Fig. 4. Number density and RMS roughness obtained from AFM.

AFM measurement. The RMS value of the pre-annealed sample is less than 0.25 nm over 5μm×5μm scan zone. With heat treatment the RMS roughness occurs due to the formation of larger QDs that lowers the number density. Interestingly, a density ~ 10^{11} cm^{-2} that is achieved using RF sputtering method is very close to the density obtained by MBE technique.

Fig.5 shows the XRD pattern of pre-annealed (lower corve) and post-annealed (upper curve) Ge nanodots. Two pronounced peaks of Ge(100) and (111) are clearly evidenced, that indicates the formation of nanosize islands. With annealing the sample, the XRD peak become sharper and full width at half-maximum (FWHM) of each peak decreases indicating that the average size of dots increases. The average size of Ge quantum dots evaluated according to Scherrer formula from XRD spectra is about 6.5 and 8.5 nm for sample A and B respectively. However, the exciton Bohr radius for Ge is 24 nm which is much larger than the size of nanoparticle suggesting the strong confinement of quantum dots that is responsible for strong PL and Raman peaks.

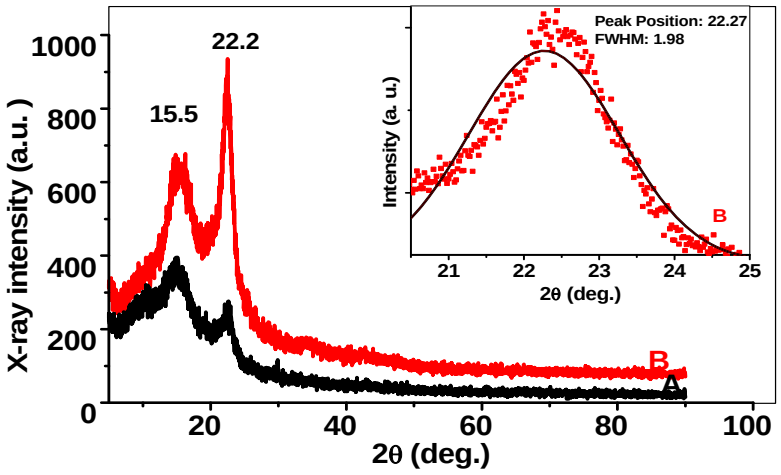

Fig. 5 The XRD pattern of pre-annealed (A) and post-annealed (B) samples.

The recorded PL spectra are presented in fig.6. The three peaks that appeared approximately at 2.85 eV and 3.21 eV and 4.13 eV indicate the interaction between Ge, GeO_x, the possibility of the formation of core-shell like structure and probably other kind of Ge nanostructure with different symmetry. Annealing the samples at 700 ^oC temperature causes the formation of larger dots, the mix state of Ge and the thicker GeO_x interface reaction that give rise to the PL peak at around 2.83 eV. Two intense peaks around 3.26 and 3.21 eV are clearly evidenced for samples A, B respectively which are attributed to the presence of Ge QDs. In nanosizing, the blue shift in the HOMO-LUMO transition energy gap becomes prominent. It is suggested that the quantum size effect that drives the visible PL shift by making the band gap nature from indirect to direct [7]. The red shift (~ 0.05 eV) of PL peak position after thermal treatment is in closed agreement with the other observations [8- 11].

Mestanza et al measured the room temperature PL spectra of Ge nanocrystalline samples on SiO_2 matrix by ion implantation technique and observed a broad blue violet band at around 3.2 eV (400 nm) originates from germanium-oxygen-deficient-centers. The occurrence of a weak peak around 4 eV is also reported [8]. The temperature dependent PL peak at 2.05 eV is observed by Sun et al [9]. A PL red shift from 1.18 to 1.05 eV is found as a function of increasing nanoparticle size from 1.6 to 9.1 nm in the experiment of Riabinina et al [10]. Three prominent PL peaks at 2.59 nm, 2.76 nm and 3.12 nm for Ge nanoparticles synthesized by the inert gas condensation (IGC) method are illustrated by Oku et al. The PL peaks are related to luminescence that originates from the Ge/GeO_x interface and quantum size effect of Ge clusters. They indicated that the formation of the core-shell structure of Ge and Si with oxide layers is the reason for blue shift of band gap energy [12]. All these studies confirm the red shift in the PL peak as observed by us. The QDs size dependent shift in the PL peak position at different annealing temperature is attributed to quantum confinement effects. The maximum of PL intensity that is observed for the sample A

with larger number density can be explained in terms of the generation of larger number of photo-carriers that contribute to the emission cross-section.

The PL peak observed at 2.85 for pre-annealed sample clearly indicates the formation of mix states and the core-shell like structure in the island. The red shift in the peak position with the annealing process is due to the formation of heavily oxidized nanoparticles as well as bigger core-shell structures. As mentioned before, the strong luminescence is due to the effect of quantum confinement in such nanoparticles. Our results confirm that the formation of core-shell structures, the presence of mix state, the quantum size and surface effects are responsible for the visible luminescence in Ge QDs.

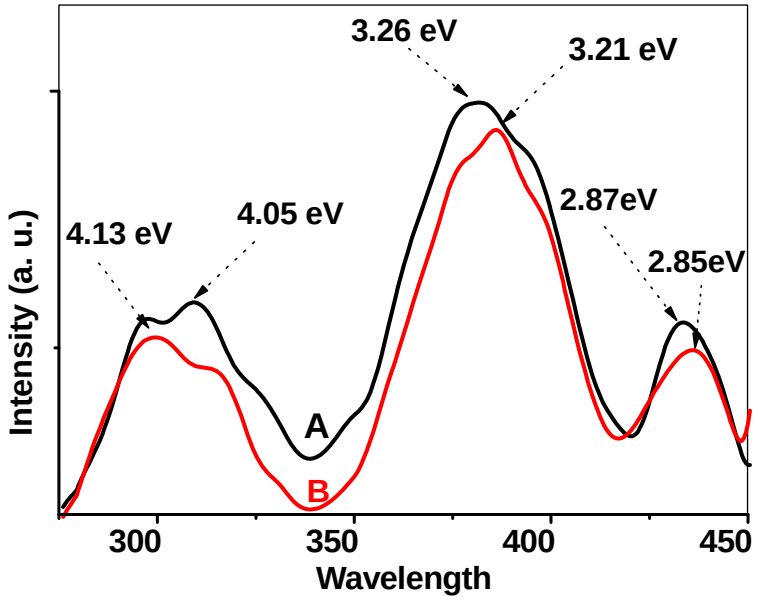

Fig. 6. The PL spectra of pre-annealed (A) and post-annealed (B) samples.

Fig.7 shows the Raman spectra of pre annealed (A) and post annealed (B) samples. The vertical dotted line fixed at 300 cm^{-1} represents the optical phonon position for bulk crystalline Ge. The frequency positions of the Ge-Ge optical phonons in QDs samples are shifted slightly to higher frequencies with respect to their bulk value. There are several possible physical mechanisms that can cause a Raman shift of optical phonons. The first one is the phonon confinement and the second one is the presence of strain. The lattice mismatch of Si and Ge leads to a compressive strain on the quantum dots in the lateral directions, which induces a Ge-Ge mode shift to the higher frequency side [10]. For the pre annealed sample three intense peaks at around 305.42, 409.19, 515.25 cm^{-1} and a weak peak at 328.68 cm^{-1} are clearly evidenced. The appearance of the broad peak at 409.19 cm^{-1} is attributed to Si-Ge vibrational mode (due to Ge-Si bonds on interface). Furthermore, the sharp but slightly asymmetric Lorantzian peak at 302.15 cm^{-1} corresponds to Ge-Ge vibration in small Ge nanocrystalline islands with phonon confinement. However, the weak peak at 329.75 cm^{-1} suggests that Ge nanocrystals must be present in GeO_x matrix. With increasing the annealing temperature, Ge-Ge and Ge-O Raman peak shift to 302.25 and 328.15 cm^{-1} respectively. The Ge-Ge optical phonon frequencies of the QDs are larger than 300 cm^{-1} but within 4.52 cm^{-1}. For the same degree of atomic inter diffusion (0.40) a small Ge-Ge mode frequency change of 3.27 cm^{-1} is attributed to the different nanodots morphology (pyramid to dome) and height-over-base ratio (0.30-0.47). The broadening of the Raman peak of the samples is attributed to phonon confinement and nanocrystal size distribution. Intensity enhancement can be related to a large portion of broken Ge-O bonds enabling a greater number of Ge atoms to participate in the larger islands formation and at the same time increasing the oxygen vacancies. The degree of the interface intermixing can be determined by the integrated peak intensity ratio

IGeGe /ISiGe because the intensity depends on the relative number of corresponding bonds as are listed in table.1. This concept is used for SiGe alloy and Ge quantum dots and can be expressed as

$$\frac{I_{GeGe}}{I_{Si-Si}} \cong B\frac{x}{2(1-x)}$$

Table 1. The average size, Ge QDs band gap energy, experimental GeGe mode frequencies and calculated Ge composition in dots.

Sample	Ave. Width (nm)	Particle diameter calculated from XRD	Band Gap Energy (eV)	W. cm^{-1} (GeGe)	Ge Comp. in dots
A	7	6.5	3.26	302.15	0.40
B	14	8.5	3.21	305.42	0.40

where x is the average Ge concentration and coefficient B is related to the Bose factor and the frequencies of GeGe and SiGe optical modes of the alloy. It is found that the coefficient B varies weakly with alloy composition and is determined to be 3.2 [13]. IGeGe/ISiGe can be obtained from fig.7.

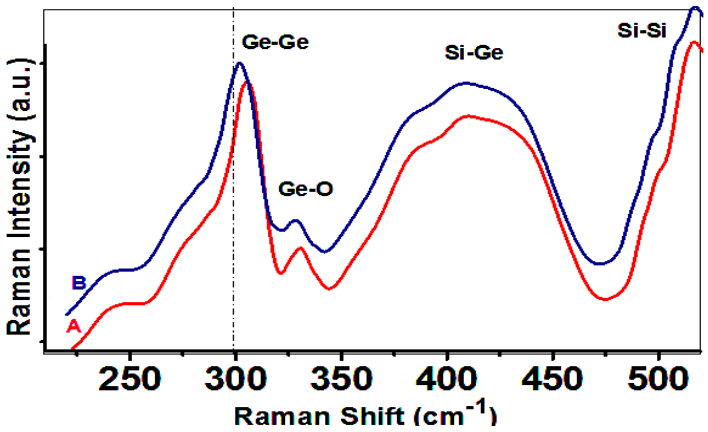

Fig. 7 Raman spectra of samples A and B.

4. Conclusions

Ge QDs are fabricated on Si(100) substrate by RF magnetron sputtering and the very high number density ~ 10^{11} cm^{-2} is obtained. The structural and optical characterizations are made by spectroscopic and inmaging techniques. The influence of annealing temperature on growth morphology, structural and optical properties is investigated in detail. Sample annealed at 700 ^{o}C exhibits larger particles ~ 14 nm which is an agreement with the theoretical results obtained by XRD Scherrer equation. Ge QDs about ~ 7 nm in diameter and 2 nm heights showed strong luminescence at 3.21 eV and the red shift (~ 0.05 eV) which is due to quantum size effect of the Ge nanoparticle. The Raman shift (~ 3.27 cm^{-1}) from pre-annealed to post-annealed sample and the broadening is attributed to the different island morphology, height-over-base ratio and phonon confinement of Ge QDs. The mechanism behind the occurrence of PL and Raman peaks and their corresponding shifts are understood. Our findings may contribute towards the development of optoelectronics devices using Ge QDs.

Acknowledgment

This work has been supported by international doctoral fellowship (IDF), Universiti Teknologi Malaysia (UTM).

References

[1] S. Huang, Z. Xia, H. Xiao, J. Zheng , Y. Xie, G. Xie, Surface & Coating Technology **204**, 558 (2009).
[2] C.N. Yea, X.M. Wua, N.Y. Tanga, L.J. Zhugea, W.G. Yaoa, J. Chenb, Y.M. Dongb, Y.H. Yub, Science and Technology of Advanced Materials **3,** 257 (2002).
[3] M. Zacharias and P. M. Fauchet, Applied Physics Letters **71**, 380 (1997).
[4] G. Kartopu, V. A Karavanskii, U. Serincan, R. Turan, R. E. Hummel, Y. Ekinci, A. Gunnæs T. G. Finstad, Physica Status Solidi A **202**, 1472-1476 (2005).
[5] V. L. Thanh, V. Yama, Y. Zhengb and D. Bouchier, Thin Solid Films, **380**, 2-9 (2000).
[6] A. F. Khan, M. Mehmood, A. M. Rana and T. Muhammad, *Applied Surface Science*, **256**, 2031-2037 (2010).
[7] T. Takagahara and K. Takeda, Physical Review B, **46**,15578 (1992).
[8] S. N. M. Mestanza, E. Rodriguez and N. C. Frateschi, Nanotechnology, **17**, 4548 (2006).
[9] K. W. Sun, S. H. Sue and C. W. Liu, Physica E, **28**, 525-530 (2005).
[10] D. Riabinina, C. Durand, M. Chaker, , Nanotechnology, **17**, 2152-2155 (2006).
[11] S. K. Ray, S. Das, R. K. Singha, S. Manna, and A. Dhar, Nanoscale Research Letters, **6**, 224-233 (2011).
[12] T. Oku , T. Nakayama , M. Kuno , Y. Nozue , L. R. Wallenberg, K. Niihara, K. Suganuma, Material and Science Engineering B, **74**, 242-247 (2000).
[13] P. M. Mooney, F. H. Dacol, J. C. Tsang and J. O. Chu, Applied Physics Letters, **62**, 2069-2071 (1993).